Field Monitoring of Avian Influenza Viruses: Whole-Genome Sequencing and Tracking of Neuraminidase Evolution Using 454 Pyrosequencing

Guillaume Croville,[a,b] Sébastien Mathieu Soubies,[a,b] Johanna Barbieri,[a,b] Christophe Klopp,[c] Jérôme Mariette,[c] Olivier Bouchez,[d,e] Christelle Camus-Bouclainville,[a,b] and Jean-Luc Guérin[a,b]

Universite de Toulouse, INP, ENVT, Toulouse, France[a]; INRA, UMR 1225, Toulouse, France[b]; Plateforme Bioinformatique Toulouse Midi-Pyrénées, UBIA, INRA, Auzeville Castanet-Tolosan, France[c]; INRA, UMR 444 Laboratoire de Génétique Cellulaire, INRA Auzeville, Castanet-Tolosan, France[d]; and GeT-PlaGe, Genotoul, INRA Auzeville, Castanet-Tolosan, France[e]

Adaptation of avian influenza viruses (AIVs) from waterfowl to domestic poultry with a deletion in the neuraminidase (NA) stalk has already been reported. The way the virus undergoes this evolution, however, is thus far unclear. We address this question using pyrosequencing of duck and turkey low-pathogenicity AIVs. Ducks and turkeys were sampled at the very beginning of an H6N1 outbreak, and turkeys were swabbed again 8 days later. NA stalk deletions were evidenced in turkeys by Sanger sequencing. To further investigate viral evolution, 454 pyrosequencing was performed: for each set of samples, up to 41,500 reads of ca. 400 bp were generated and aligned. Genetic polymorphisms between duck and turkey viruses were tracked on the whole genome. NA deletion was detected in less than 2% of reads in duck feces but in 100% of reads in turkey tracheal specimens collected at the same time. Further variations in length were observed in NA from turkeys 8 days later. Similarly, minority mutants emerged on the hemagglutinin (HA) gene, with substitutions mostly in the receptor binding site on the globular head. These critical changes suggest a strong evolutionary pressure in turkeys. The increasing performances of next-generation sequencing technologies should enable us to monitor the genomic diversity of avian influenza viruses and early emergence of potentially pathogenic variants within bird flocks. The present study, based on 454 pyrosequencing, suggests that NA deletion, an example of AIV adaptation from waterfowl to domestic poultry, occurs by selection rather than *de novo* emergence of viral mutants.

A critical biological feature of influenza viruses, shared with all RNA viruses, is their high genetic variability generated by poor proofreading activity. As a consequence, influenza viruses appear as clouds of mutants, referred to as quasispecies, which can hardly be assessed by a consensus sequence (15). Deep sequencing is therefore an alternative approach to dissecting this genetic complexity by detecting minority mutants in complex viral populations.

Low-pathogenicity avian influenza virus (LPAIV) infections in poultry are mostly nonclinical and therefore remain poorly investigated despite the role of precursors of highly pathogenic (HP) strains.

The presence of a polybasic cleavage site in the hemagglutinin (HA) sequence is known as the main support of pathogenicity in avian hosts. However, determinants involved in the adaptation to gallinaceous birds have also been identified. Examples of such determinants are represented by deletions in the stalk of the neuraminidase (NA), which occur during viral circulation in poultry. These deletions appear to contribute to viral adaptation to these species (13, 16) and to a change in viral tropism from the intestine to the respiratory tract of birds (23). Reverse genetic studies recently confirmed that NA stalk deletions are associated with an increased virulence in poultry (17, 20, 24). These deletion events have been recurrently observed in viral isolates infecting gallinaceous birds and are phylogenetically close to strains circulating in wild birds (2, 4). Nevertheless, parental and truncated viruses have not been tracked thus far in field conditions.

In this study, we investigate a case of H6N1 infection in Muscovy ducks, which resulted in in-farm contamination of turkeys, and monitored genetic changes on the 8 viral segments. A partic-

ular interest was focused on NA: using deep sequencing, we were able to detect ultraminority deleted NA alleles in ducks, which were found in 100% of NA sequences in turkeys, and then evolved further with cocirculation of 2 forms of NA deletions in the same birds. Altogether, these results illustrate the invaluable contribution of deep sequencing to the fine dissection of genetic species of influenza viruses.

MATERIALS AND METHODS

Clinical examination and sampling of birds. The poultry farm, localized in Pays de la Loire, France, included 2 sheds, which housed, at the time of the infectious episode in March 2009, 8,700 Muscovy ducks and 8,000 meat turkey poults, respectively. The 2 sheds were totally closed, bird-proofed, and independently cared for by the same farmer. On the first day of a clinical episode, a sampling of 10 diseased turkeys was performed, and at the same time, several samples of fecal material in the duck house were collected and pooled. A second necropsy was performed on 10 birds 8 days after the first one. Tracheal swabs and organ samples were taken from all dead animals. Swabs were immediately stored at −80°C until further pro-

TABLE 1 Comparison of nucleotide and amino acid sequences of A/Muscovy duck/France/09010/09(H6N1) with A/turkey/France/09010–1/09(H6N1) and A/turkey/France/09010–2/09(H6N1) viruses

Segment	Protein	A/Turkey/France/09010–1/09(H6N1)			A/Turkey/France/09010–2/09(H6N1)		
		Nucleotide identity (%)	Amino acid identity (%)	Amino acid changes	Nucleotide identity (%)	Amino acid identity (%)	Amino acid changes
1	PB2	2,005/2,280 (87.9)	751/759 (98.9)	R61K, T147I, V292I, V295I V397A, I511V, T585P, D680G	2,005/2,280 (87.9)	751/759 (98.9)	R61K, T147I, V292I, V295I V397A, I511V, T585P, D680G
2	PB1	2,190/2,274 (96.3)	750/757 (99)	K52N, R54K, A56T, M195I, L550I, R584H, N694S	2190/2274 (96.3)	750/757 (99)	K52N, R54K, A56T, M195I, L550I, R584H, N694S
	PB1-F2	258/273 (94.5)	76/90 (84.4)	E4G, R21 M, G22E, G23S, Q26R, L30P, T46 M, Q48R, A49V, K53R, Q54R, K65R, Q79R, S82L	258/273 (94.5)	76/90 (84.4)	E4G, R21 M, G22E, G23S, Q26R, L30P, T46 M, Q48R, A49V, K53R, Q54R, K65R, Q79R, S82L
3	PA	2,059/2,151 (95.7)	714/716 (99.7)	A70V, E538G	2,059/2,151 (95.7)	714/716 (99.7)	A70V, E538G
4	HA	1,698/1,701 (99.8)	565/566 (99.8)	K118R	1,698/1,701 (99.8)	565/566 (99.8)	K118R
5	NP	1,497/1,497 (100)	498/498 (100)		1,497/1,497 (100)	498/498 (100)	
6	NA	1,350/1,350 (excluding deletion)	449/449 (100)	N.B.: amino acids 55–74 are absent in the turkey isolate (deleted region)	1,350/1,350 (excluding deletion)	449/449 (100)	N.B.: amino acids 55–74 are absent in the turkey isolate (deleted region)
					1,341/1,341 (excluding deletion)	446/446 (100)	N.B.: amino acids 43–66 are absent in the turkey isolate (deleted region)
7	M1	759/759 (100)	252/252 (100)		759/759 (100)	252/252 (100)	
	M2	294/294 (100)	97/97 (100)		294/294 (100)	97/97 (100)	
	NS1	693/693 (100)	230/230 (100)		693/693 (100)	230/230 (100)	
8	NEP	366/366 (100)	121/121 (100)		366/366 (100)	121/121 (100)	

cessing. Histological examination of the trachea and lung of turkeys was performed using routine procedures.

RNA extraction and RT-PCR. All the swabs received at the National Veterinary School of Toulouse were first vortexed in a 500-µl PBS solution. Viral RNA was extracted from 150 µl of sample by use of the RNA Virus kit (Macherey-Nagel, Düren, Germany) according to the manufacturer's protocol. The RNA was eluted into 50 µl RNase-free water. Each of the viral gene segments was amplified by 2-step reverse transcription-PCR (RT-PCR). For reverse transcription, 20 µl of total RNA was mixed with 40 pmol of Uni12 primer (7) and incubated for 5 min at 65°C. Then, 8 µl of 5× reaction buffer (Fermentas, Glen Burnie, MD) was added to this mixture at the same time as 1 µl of RiboLock RNase inhibitor (Fermentas), 4 µl of 10 mmol/liter deoxynucleoside triphosphate (dNTP) solution (Finnzymes, Espoo, Finland), and 2 µl of RevertAid reverse transcriptase (Fermentas). The reaction volume was completed to 40 µl with distilled water. The RT reaction was performed at 42°C for 60 min and terminated by heating at 70°C for 10 min.

cDNAs were amplified by using Phusion High-Fidelity DNA polymerase (Finnzymes) and a set of gene-specific primers (7).

Eight separated PCR mixtures, corresponding to the 8 genes, were prepared and contained 29.5 µl of distilled water, 10 µl of 5× buffer, 1 µl of 10 mmol/liter dNTP solution (Finnzymes), 2.5 µl of 10 µmol/liter primers, 4 µl of the cDNA, and 1 unit Phusion High-Fidelity DNA polymerase. The amplification program consisted of a first 30-s step at 98°C followed by 35 cycles with the following conditions: 98°C for 10 s, 61°C for 20 s, and 72°C for 1 min 30 s. The program ended with 1 step at 72°C for 10 min.

Sanger sequencing of the amplification products. The amplification products were separated by electrophoresis using 1% agarose gels. Observed bands were excised from the gel and purified using the Nucleospin Extract II kit (Macherey-Nagel) according to the manufacturer's protocol. These PCR products were eluted into 50 µl of distilled water and subsequently used in Sanger sequencing and pyrosequencing. By Sanger sequencing, we determined consensus whole-genome sequences for each of the 3 types of sampling.

Differential real-time PCR on neuraminidase alleles. Quantitative real-time PCR was also used to characterize the neuraminidase allele(s) present in duck feces or turkey tracheas. A set of primers and probes was designed for full-length neuraminidase or truncated neuraminidase detection, according to the Sanger sequencing results. The forward primer was NA-F (5′-AGACAGGGAATCAGCACCAG-3′), and the reverse primer was Delta-R (5′-TTGGGCAAAGAGATGCATTA-3′). The TaqMan probe sequences targeting the complete or the truncated NA were 5′-FAM-TGAAAACAACACTTGGGTAAATCAGACC-BHQ-3′ and 5′-JOE-AAAAGCATCATTCTTACTGAGCAAGCTGT-BHQ-3′, respectively. Both were coupled with a Black Hole Quencher dye at the 3′ end. Viral RNA was retrotranscribed as described before, and cDNA was amplified and detected in a 7000 Sequence Detection System (PE Applied Biosystems) by using the Platinum Quantitative PCR SuperMix-UDG (Invitrogen SRL, Milan, Italy). The 25-µl PCR mixture contained 5 pmol of each primer and 50 pmol probe. After 2 thermal steps at 50°C for 2 min and 95°C for 2 min, 40 cycles of PCR at 95°C for 15 s and at 60°C for 30 s were performed.

454 pyrosequencing of the amplification products. The previously purified PCR products were quantified using a Quant-iT PicoGreen kit (Molecular Probes, Eugene, OR). Libraries were prepared after PCR product nebulization using the GS DNA Rapid Library Preparation kit according to the manufacturer's recommendations (Roche, Basel, Switzerland). Three pools (corresponding to the 3 different sets of samplings), each containing 500 ng DNA, were used to generate the libraries; the 8 segments were pooled in equimolar amounts. Each DNA pool was ligated to an adapter containing a multiplex identifier sequence (MID) for emulsion PCR and sequencing. Final libraries were quantified using the SlingShot kit, using the Fluidigm Digital Array for sample quantification, following the manufacturer's instructions. Pyrosequencing using the 454/Roche GS
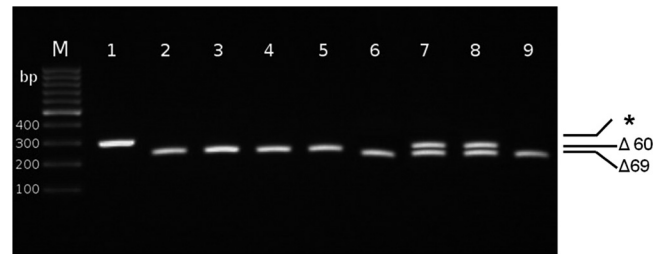
FIG 1 Typical agarose gel electrophoresis pattern of NA gene-specific RT-PCR products from duck and turkey clinical specimens, using internal primers (NA-F: 5′-TGGTAATTGGAATAGTCAGTTTGA-3′; NA-R: 5′-ATCCCCTT TGGAACCAATTC-3′). Lane 1: duck feces; lanes 2 to 5: representative early turkey swabs, showing a 60-nucleotide deletion; lanes 6 to 9: representative late turkey swabs, showing various, mixed patterns of deletion. M: molecular mass marker; *: full-length NA. Δ60 and Δ 69: 60-nt and 69-nt deletion, respectively.

FLX Titanium chemistry was carried out with the GS Titanium SV emulsion PCR kit and sequencing kit according to the manufacturer's instructions. The 3 samples were sequenced on 1 region of an 8-region picotiter plate.

Bioinformatic analysis. Sequences were first demultiplexed using Roche's tool SFF file without allowing any error per MID. Reads were then filtered using pyrocleaner (14), considering different criteria such as length. Reads shorter or longer than the mean length of the reads ±2 standard deviations were discarded. Reads were also filtered based on their complexity, which is computed using the compressed string length (library zip) on several subsequences generated using a sliding window approach. Moreover, the pyrocleaner script removes sequences for which all base pairs have a phred quality value under 20 or if the rate of undetermined bases is higher than 4%, which has been proven to correlate with poor quality. Next, to carry out the single nucleotide polymorphism (SNP) calling, the remaining sequences were assembled on the reference to produce a consensus sequence for each sample. To do so, sequences were aligned against the reference genome using bwa (11), and the consensus was computed with the SAMtools (12) software package. Reads were then realigned against this consensus sequence before SNP calling using other modules of the same package. For large deletion discovery, the BLAT (10) aligner was used on the same reads for each sample. The resulting files were then displayed within the IGV (22) browser.

Nucleotide sequence accession numbers. The complete sequences of A/Muscovy duck/France/09010/09, A/turkey/France/09010–1/09, and A/turkey/France/09010–2/09 (H6N1) viruses have been deposited in GenBank under accession numbers JN860169 to JN860193.

RESULTS

Case history and virological findings. Three days after the removal of ducks to the slaughterhouse, the turkey flock started to show prostration and respiratory signs, resulting in approximately 10% mortality. A sampling of 10 diseased turkeys was performed, and at the same time, several samples of fecal material in the duck house were collected and pooled. Necropsies were performed on the 10 birds, and all showed severe exudative tracheitis, airsacculitis, and pneumonia. A routine antibiotic treatment was performed to prevent secondary bacterial infections, but it did not stop mortality. A second necropsy was therefore performed on 10 other birds 8 days later. Tracheal swabs and organ samples were taken from all dead animals.

Real-time PCR assays were negative for *Mycoplasma gallisepticum* and *Mycoplasma synoviae*. Real-time RT-PCR analyses of the tracheal samples were negative for avian metapneumovirus (5) but positive for avian influenza virus (AIV) (3).

Croville et al.

TABLE 2 Quantitative RT-PCR distinguishing between wild-type and truncated NA[a]

		Mean no. of copies ± SD	
Specimen type	Probe sequence	Wild-type NA	Truncated NA
Duck feces	TGAAAACAACACTTGG GTAAATCAGACC	787 ± 311	ND
Turkey swabs	AAAAGCATCATTCTTA CTGAGCAAGCTGT	ND	5,109 ± 1,585

[a] ND, not detected. 5′ primer sequence AGACAGGGAATCAGCACCAG; 3′ primer sequence, TTGGGCAAAGAGATGCATTA.

Immunostaining for influenza virus A revealed infected cells in the tracheal epithelium and in the pulmonary parenchyma at the time of the first sampling (data not shown).

Sequence analysis of duck and turkey isolates. RT-PCR am-

plifications encompassing all the viral genomic segments' coding sequences were performed on both turkey tracheal swabs and duck feces using a set of gene-specific primers for influenza viruses (7). This procedure, followed by Sanger sequencing, led to the identification of the H6N1 subtype. Comparison of complete sequences of duck and turkey viruses (Table 1) revealed more than 99.8% nucleotide (nt) identity genome-wide, except for (i) one internal deletion of 60 nt in segment 6 resulting in a putative 20-aa deletion in the neuraminidase stalk in all of the first turkey isolates collected and (ii) a singular pattern of NA stalk deletions consisting of a mix of the 60-nt deleted allele and a new, second 69-nt deleted one in some turkeys swabbed after 8 days of infection, as confirmed by cloning and sequencing. Four of 10 birds sampled at this later stage of infection in the turkey barn showed this mixed pattern (representative specimens shown in Fig. 1).

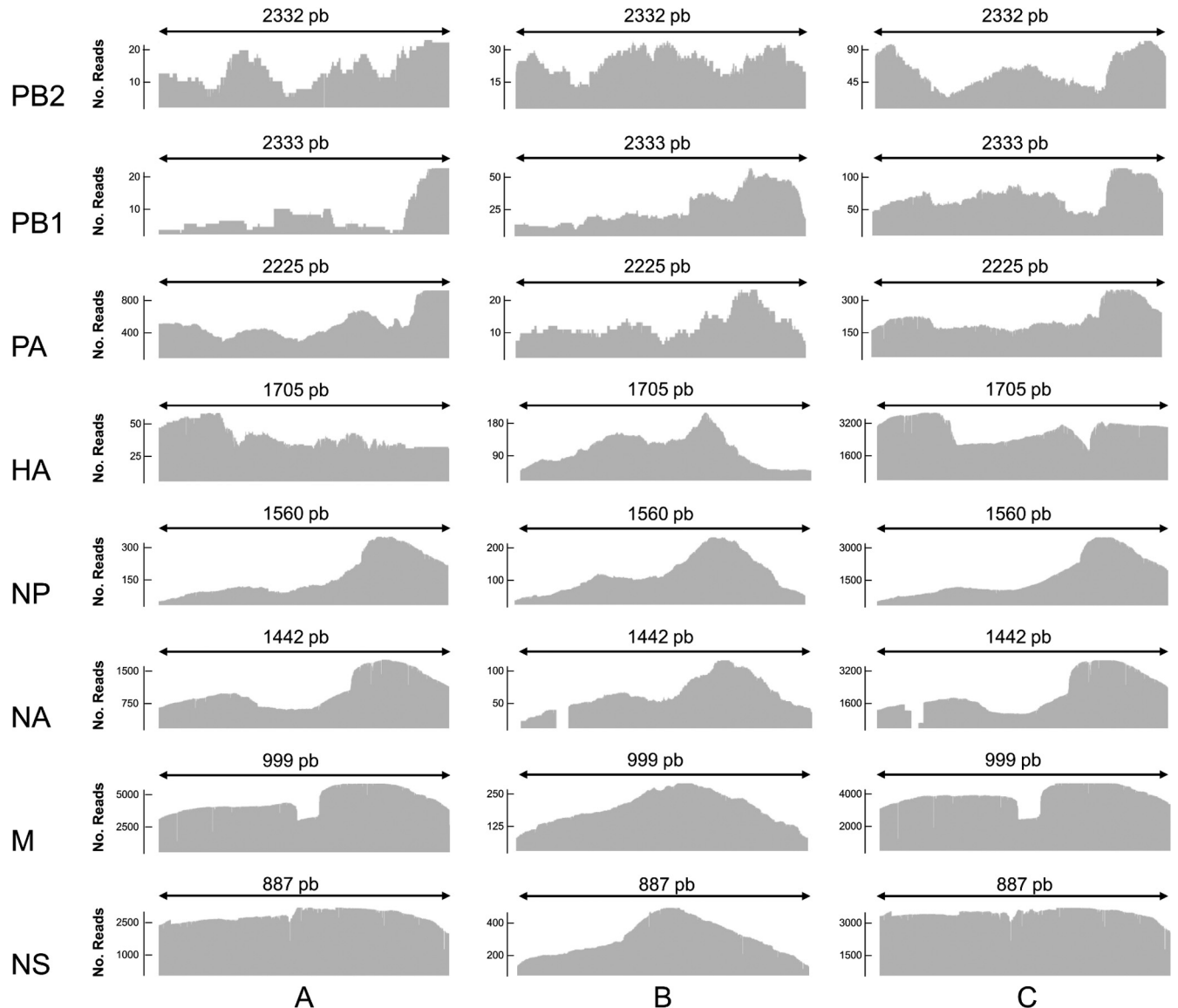**Differential real-time PCR on Neuraminidase alleles.** To deter-

FIG 2 Map of sequence depth of the whole influenza genome for duck (A), early turkey (B), and late turkey virus (C). For each segment, the coverage depth is plotted as a function of nucleotide position. PA: PA polymerase; HA: hemagglutinin; NP: nucleoprotein; NA: neuraminidase; M: matrix; NS: nonstructural.

TABLE 3 Nonsynonymous single nucleotide polymorphisms (SNPs) detected on PB2 and HA[a]

Protein	Nucleotide			Protein			Population ratio (%)		
	Base(s)	Position	Substitution	Amino acid	Position	Substitution	A	B	C
PB2	AGA	181	AAG	R	61	K	0	95	95
	C	300	A	N	100	K	0	0	8
	A	346	C	K	116	Q	0	0	5
	A	361	G	K	121	E	0	7	10
	C	440	T	T	147	I	0	100	100
	A	563	G	E	188	G	25	0	0
	A	569	G	K	190	R	23	0	0
	G	571	A	E	191	K	21	0	0
	G	874	A	V	292	I	0	100	100
	GTG	883	ATT	V	295	I	0	100	100
	GTG	1189	GCA	V	397	A	0	100	100
	G	1261	A	V	421	I	0	0	23
	ATT	1531	GTA	I	511	V	0	100	100
	CCT	1735	ACA	P	579	T	0	14	0
	ACT	1753	CCC	T	585	P	25	100	100
	AAG	1756	CAA	K	586	Q	0	7	14
	GAT	2038	GGC	D	680	G	0	100	100
HA	A	353	G	K	118	R	0	100	62
	C	358	T	L	120	F	6	0	0
	A	509	G	K	170	R	0	0	6
	G	534	T	K	178	N	9	0	0
	A	560	T	Q	187	L	0	0	38
	G	685	A	E	229	K	0	0	25
	C	692	T	A	231	V	0	0	25
	G	722	C	G	241	A	0	0	14
	T	1004	C	L	335	P	0	0	20
	C	1041	A	F	347	L	0	0	6
	T	1262	C	I	421	T	0	0	23

[a] For each library, corresponding to duck feces (A), early samples in turkeys (B), and late samples in turkeys (C), reads were aligned against the consensus sequence before SNP calling. The percentage of reads sharing the SNP was determined with a threshold of 5%.

mine if the deleted forms were present, even at low copy number, in duck feces samplings, a real-time PCR assay was designed to discriminate between undeleted and deleted NA, using a unique couple of primers encompassing the deletion region of NA and 2 sequence-specific internal probes (Table 2). The copy number was deduced from a plasmidic standard dilution (ranging from 10 to 10^6 copies) containing the cognate sequences. This allele-specific real-time PCR showed a very low threshold of less than 10 copies per reaction (data not shown) and was performed in triplicate on duck and turkey samples. Using this sensitive method, we readily detected the full-length NA but not the truncated segment in duck samples. The same analysis, when applied to early turkey tracheal swabs, only detected the truncated form of the NA segment (Table 2).

Deep sequencing of complete viral genome of duck and turkey viruses. Complete genomes were obtained for the 3 pools of samples, with a mean number of reads of 21,600 per pool and an average coverage depth of 680 for all segments. A comprehensive coverage map is shown in Fig. 2.

For each viral gene, SNPs were tracked on the basis of a 5% threshold. Table 3 summarizes the nonsynonymous SNPs and the ratio of mutated viral sequences for PB2 and HA. Briefly, 8 SNPs on PB2 appeared within a few days in 100% of the turkey viral reads. Some minority mutants in the ducks disappeared as readily as in the turkeys. On HA, one SNP (K118R) was identified and remained preponderant in turkeys in the late samples. Eight other minority SNPs, concerning 6% to 32% of the reads, were evi-

denced in late samples on positions 170 to 241, corresponding to the receptor binding region of HA. Data concerning the 6 other segments are shown in Table SA1 in the supplemental material; SNPs were observed in turkeys on PB1 (7 positions), PB1-F2 (14 positions), and PA (3 positions).

A particular analysis was performed on the NA gene; as expected, we identified a 100% 60-nt deleted population in early turkey samples and a mixed 60- and 69-nt deletion pattern in late turkey samples. Alignments of the NA genes could readily evidence a comprehensive pattern of deletions (Fig. 3). More surprising is that the same analysis on duck fecal material evidenced an ultraminority population of deleted 60-nt NA alleles (13/670 reads, i.e., 1.94%), which was not detected by other means (Fig. 3). This critical result demonstrates that minute amounts of deleted NA alleles were present in the duck viral mutant cloud and "emerged" in the turkeys.

DISCUSSION

In this study, we monitored the evolution of LPAIVs by pyrosequencing performed directly on clinical samples. The whole genomes of 3 pooled samples were subjected to deep sequencing and analysis of viral subpopulations. The global sequence coverage was sufficient to observe low population variation, which may possibly represent quasispecies, and to track the evolution of minority mutants. For this purpose, a critical advantage of 454 pyrosequencing, when compared with other next-generation sequencing platforms, relies on its ability to generate quite long
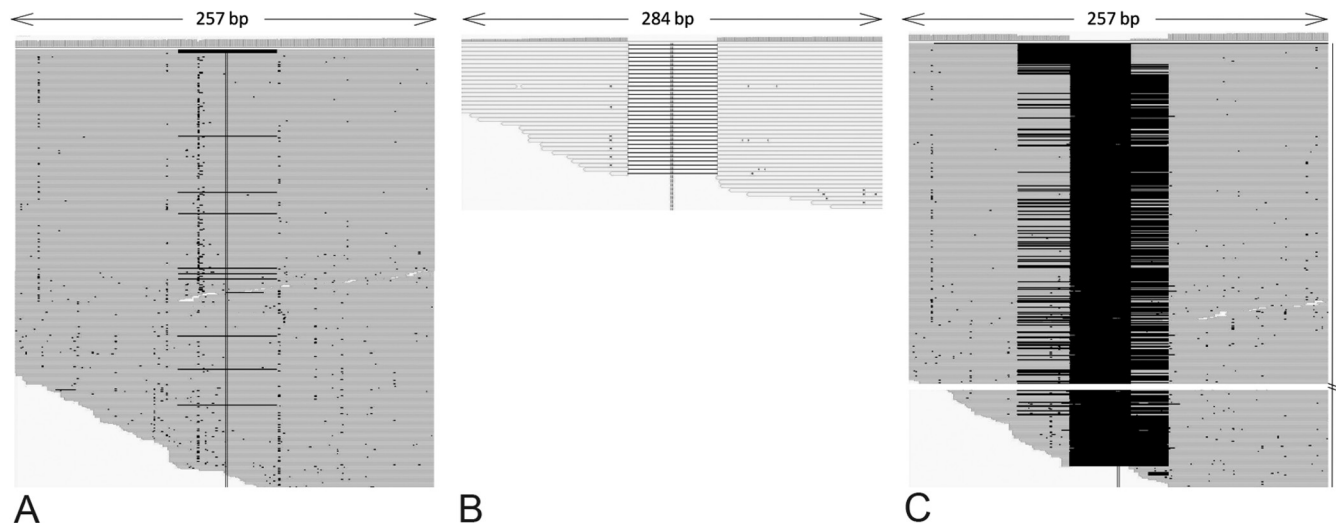
FIG 3 Read alignments on the NA stalk region, focusing on deletion patterns; 454 reads were contiged and aligned. Deletion in the stalk region (positions 161 to 220) was found in only 13 of 670 reads in duck feces (A) but in 100% of reads in early samples from turkeys (B). A mix of 60- and 69-nt (positions 129 to 197) deletions was observed in turkeys 8 days later (C).

reads, of roughly 400 nt (at the time of the experiment), facilitating subsequent sequence reconstruction.

One of the most significant changes observed was the emergence of 2 avian influenza NA stalk deletion variants after virus transmission from the ducks to the turkeys. In this case study, the NA stalk deletions could be monitored in the field, at the scale of a single farm, with a direct link from the parental to the deletion variants.

Our data favor the idea that NA stalk truncation emerged early after turkey contamination, as a minute number of reads of deleted NA could be detected in duck feces. Besides, we did not detect any full-length NA form in turkeys, even in early samples, suggesting a strong evolutionary advantage of the truncated form at the expense of the full-length one in this poultry species.

Very surprising is that after 8 more days of viral circulation in turkeys, some birds appeared to be coinfected with a second variant harboring a larger deleted region, which did not totally overlap with the 60-nt deletion previously observed. This later Δ69 allele could not be detected in early turkey samples, maybe because the depth coverage of NA was quite low for this early sample. This finding suggests a higher plasticity of neuraminidase than previously thought.

NA stalk truncation events, which reduce the protein enzymatic activity, have been shown to be associated with changes in the glycosylation pattern of the HA globular head, resulting in a modification of HA affinity for cellular receptors (5, 17, 19).

We tracked the evolution of HA and could evidence the emergence of minority mutants, with substitutions mostly in the receptor binding site on the globular head: these SNPs concerned up to 38% of viral species after 8 days of clinical evolution in the flock. None of these mutations altered glycosylation sites of HA. They may have contributed to the refinement of binding to cellular receptors of the turkeys' upper respiratory tract and/or to circumvent the host's immune response (18).

It is of interest to note that the observed mortality in turkeys was contemporary to NA deletion variant detection, whereas ducks did not show any clinical sign of infection. Even though NA stalk deletion was recently associated with an increased virulence in chickens infected by reverse-genetics-engineered viruses (8, 20), whether the deletions described in this field case are responsible for the observed virulence in turkey remains to be demonstrated.

In this farm, the 2 species were bred separately in 2 different houses. The contamination of turkeys can likely be explained by a biosecurity failure, which probably occurred when ducks were transported to the slaughterhouse. This case suggests further that the turkey is a very peculiar host among poultry species and shows very high receptivity and sensitivity to influenza A viruses (21). Recent epidemiological modeling data suggest a very high within-flock transmissibility of LPAIVs in turkeys (1). This case also emphasizes the risks of breeding together different avian species, i.e., terrestrial birds (chickens or turkeys) and waterfowl. Such a situation, which seems relatively common in Asia, can result in the quick emergence of variants with altered phenotypes and increased pathogenicity. Moreover, it illustrates the genetic heterogeneity of avian influenza viruses within a single flock. In a first attempt, our approach was intentionally based on the poultry population considered as a whole, irrespective of the individual level. The next step will be to investigate quasispecies variations between birds in a flock and then between different tissues (i.e., respiratory versus digestive tracts) in given birds.

In previous studies, next-generation sequencing approaches have already proven to be of interest for monitoring viral evolution at precise viral genome positions following evolutionary constraints such as antiretroviral treatment during HIV infection (6) or oseltamivir treatment during influenza infection (9). A broader approach of viral genome evolution may allow us to monitor the early apparition of mutants without a priori consideration and to follow complex chains of mutational events occurring on several positions of viral genomes. The 454 sequencing platform used here has the critical advantage of producing long reads—from 400 nt to more than 700 nt in recent updates—facilitating sequence reconstruction in a whole viral genome approach. Alternative technologies are in constant development and will likely provide

improved sequencing capacities in the near future. The development of next-generation sequencing approaches should enable us to monitor both viral genome diversity within bird flocks and the early apparition of potentially pathogenic variants.

Although our data do not explain how the NA stalk deletion appeared in the duck samples in the first place, this present study suggests that this deletion can exist as a minority mutant in waterfowl, awaiting a change of host to be selected.

ACKNOWLEDGMENTS

REFERENCES

1. **Comin A, Klinkenberg D, Marangon S, Toffan A, Stegeman A.** 2011. Transmission dynamics of low pathogenicity avian influenza infections in Turkey flocks. PLoS One **6:**e26935.

2. **Di Trani L, et al.** 2004. Molecular characterization of low pathogenicity H7N3 avian influenza viruses isolated in Italy. Avian Dis. **48:**376–383.

3. **Fouchier RA, et al.** 2000. Detection of influenza A viruses from different species by PCR amplification of conserved sequences in the matrix gene. J. Clin. Microbiol. **38:**4096–4101.

4. **Giannecchini S, et al.** 2006. Comparison of in vitro replication features of H7N3 influenza viruses from wild ducks and turkeys: potential implications for interspecies transmission. J. Gen. Virol. **87:**171–175.

5. **Guionie O, et al.** 2007. Laboratory evaluation of a quantitative real-time reverse transcription PCR assay for the detection and identification of the four subgroups of avian metapneumovirus. J. Virol. Methods **139:**150–158.

6. **Hedskog C, et al.** 2010. Dynamics of HIV-1 quasispecies during antiviral treatment dissected using ultra-deep pyrosequencing. PLoS One **5:**e11345.

7. **Hoffmann E, Stech J, Guan Y, Webster RG, Perez DR.** 2001. Universal primer set for the full-length amplification of all influenza A viruses. Arch. Virol. **146:**2275–2289.

8. **Hoffmann TW, et al.** 2012. Length variations in the NA stalk of an H7N1 influenza virus have opposite effects on viral excretion in chickens and ducks. J. Virol. **86:**584–588.

9. **Inoue M, et al.** 2010. Emergence of oseltamivir-resistant pandemic (H1N1) 2009 virus within 48 hours. Emerg. Infect. Dis. **16:**1633–1636.

10. **Kent WJ.** 2002. BLAT: the BLAST-like alignment tool. Genome Res. **12:**656–664.

11. **Li H, Durbin R.** 2009. Fast and accurate short read alignment with Burrows-Wheeler transform. Bioinformatics **25:**1754–1760.

12. **Li H, et al.** 2009. The Sequence alignment/map format and SAMtools. Bioinformatics **25:**2078–2079.

13. **Li J, Zu Dohna H, Cardona CJ, Miller J, Carpenter TE.** 2011. Emergence and genetic variation of neuraminidase stalk deletions in avian influenza viruses. PLoS One **6:**e14722.

14. **Mariette J, Noirot C, Klopp C.** 2011. Assessment of replicate bias in 454 pyrosequencing and a multi-purpose read-filtering tool. BMC Res. Notes **4:**149.

15. **Mathieu C, et al.** 2010. Pandemic (H1N1) 2009 in breeding turkeys, Valparaiso, Chile. Emerg. Infect. Dis. **16:**709–711.

16. **Matrosovich M, Zhou N, Kawaoka Y, Webster R.** 1999. The surface glycoproteins of H5 influenza viruses isolated from humans, chickens, and wild aquatic birds have distinguishable properties. J. Virol. **73:**1146–1155.

17. **Matsuoka Y, et al.** 2009. Neuraminidase stalk length and additional glycosylation of the hemagglutinin influence the virulence of influenza H5N1 viruses for mice. J. Virol. **83:**4704–4708.

18. **McHardy AC, Ben Adams B.** 2009. The role of genomics in tracking the evolution of influenza A virus. PLoS Pathog. **5:**e1000566.

19. **Mitnaul LJ, et al.** 2000. Balanced hemagglutinin and neuraminidase activities are critical for efficient replication of influenza A virus. J. Virol. **74:**6015–6020.

20. **Munier S, et al.** 2010. A genetically engineered waterfowl influenza virus with a deletion in the stalk of the neuraminidase has increased virulence for chickens. J. Virol. **84:**940–952.

21. **Pillai SPS, Pantin-Jackwood M, Yassine HM, Saif YM, Lee CW.** 2010. The high susceptibility of turkeys to influenza viruses of different origins implies their importance as potential intermediate hosts. Avian Dis. **54:**522–526.

22. **Robinson JT, et al.** 2011. Integrative genomics viewer. Nat. Biotechnol. **29:**24–26.

23. **Sorrell EM, Song H, Pena L, Perez DR.** 2010. A 27-amino-acid deletion in the neuraminidase stalk supports replication of an avian H2N2 influenza A virus in the respiratory tract of chickens. J. Virol. **84:**11831–11840.

24. **Zhou H, et al.** 2009. The special neuraminidase stalk-motif responsible for increased virulence and pathogenesis of H5N1 influenza A virus. PLoS One **4:**e6277.